


Machine learning applied to atopic dermatitis transcriptome reveals distinct therapy-dependent modification of the keratinocyte immunophenotype*

K. Clayton ¹, A. Vallejo,¹ S. Sirvent,¹ J. Davies,¹ G. Porter,¹ I.C. Reading,^{2,3} F. Lim,⁴ M.R. Ardern-Jones^{1,5} and M.E. Polak ^{1,6}

¹Department of Clinical and Experimental Sciences (Sir Henry Wellcome Laboratories, Faculty of Medicine)

²Department of Primary Care and Population Sciences (Faculty of Medicine)

³NIHR, Research Design Service South Central, Southampton, Hants, UK

⁴Unilever Research, Colworth Science Park, Sharnbrook, Bedfordshire, UK

⁵Department of Dermatology, University Hospital Southampton NHS Foundation Trust, Southampton, Hants, UK

⁶Institute for Life Sciences, University of Southampton, Southampton, Hants, UK

Linked Comment: Miyano and Tanaka. *Br J Dermatol* 2021; **184**:798–799.

Summary

Correspondence

Marta E. Polak.

Email: m.e.polak@soton.ac.uk

Accepted for publication

23 July 2020

Funding sources

This work was supported by the Medical Research Council DTP PhD scheme and iCASE partnership with Unilever (scheme no. MR/N014308/1).

M.E.P. is funded by a Sir Henry Dale Fellowship, Wellcome Trust (grant no. 10937/Z/15/Z).

Conflicts of interest

The authors declare they have no conflict of interest.

M.R.A.-J. and M.E.P. contributed equally.

*Plain language summary available online

DOI 10.1111/bjd.19431

Background Atopic dermatitis (AD) arises from a complex interaction between an impaired epidermal barrier, environmental exposures, and the infiltration of T helper (Th)1/Th2/Th17/Th22 T cells. Transcriptomic analysis has advanced our understanding of gene expression in cells and tissues. However, molecular quantitation of cytokine transcripts does not predict the importance of a specific pathway in AD or cellular responses to different inflammatory stimuli.

Objectives To understand changes in keratinocyte transcriptomic programmes in human cutaneous disease during development of inflammation and in response to treatment.

Methods We performed *in silico* deconvolution of the whole-skin transcriptome. Using co-expression clustering and machine-learning tools, we resolved the gene expression of bulk skin (seven datasets, $n = 406$ samples), firstly, into keratinocyte phenotypes identified by unsupervised clustering and, secondly, into 19 cutaneous cell signatures of purified populations from publicly available datasets. **Results** We identify three unique transcriptomic programmes in keratinocytes – KC1, KC2 and KC17 – characteristic of immune signalling from disease-associated Th cells. We cross-validate those signatures across different skin inflammatory conditions and disease stages and demonstrate that the keratinocyte response during treatment is therapy dependent. Broad-spectrum treatment with ciclosporin ameliorated the KC17 response in AD lesions to a nonlesional immunophenotype, without altering KC2. Conversely, the specific anti-Th2 therapy, dupilumab, reversed the KC2 immunophenotype.

Conclusions Our analysis of transcriptomic signatures in cutaneous disease biopsies reveals the effect of keratinocyte programming in skin inflammation and suggests that the perturbation of a single axis of immune signal alone may be insufficient to resolve keratinocyte immunophenotype abnormalities.

What is already known about this topic?

- Atopic dermatitis (AD) is a complex interaction of impaired epidermal barrier, environmental exposures and the infiltration of T helper (Th)1/Th2/Th17/Th22 T cells.

- However, molecular quantitation of cytokine transcripts does not predict the importance of a specific pathway in AD or cellular responses to different inflammatory stimuli.
- A macro view of the AD transcriptome prevents characterization of individual responses of the various cell types comprising skin.

What does this study add?

- *In silico* deconvolution of the whole-skin transcriptome identified three keratinocyte (KC)-transcriptomic programmes: KC1 (interferon response), KC2 [interleukin (IL)-4 and IL-13 responses] and KC17 (IL-17 response).
- Ciclosporin ameliorated the KC17 response in AD lesions to a nonlesional immunophenotype, without altering KC2. Dupilumab reversed the KC2 immunophenotype.

What is the translational message?

- Our analysis reveals the complexity of keratinocyte programming in skin inflammation, suggesting the perturbation of a single axis of immune signal alone may be insufficient to resolve keratinocyte abnormalities.

Atopic dermatitis (AD) arises from complex interactions between an impaired epidermal barrier and environmental exposures to allergens and irritants, resulting in aberrantly activated infiltrating immune cells. Much interest has focused on the immune cells infiltrating AD skin, which mediate disease. In particular, dense infiltration of activated T helper (Th)2/Th22 CD4⁺ T cells is an early feature of AD exacerbations, especially in acute lesions.¹ These are identified also in nonlesional skin of AD sufferers suggesting a systemic immunodysregulation.^{2,3} This implies that type 2 cytokines play a major role in disease pathogenesis and clinical research has shown the impressive efficacy in AD treatment of a monoclonal antibody therapy targeting interleukin (IL)-4 (receptor α subunit) R α , which blocks IL-4 and IL-13 signalling.⁴ However, studies by Gittler *et al.* first demonstrated that the Th1/Th17 axis is also prominent in chronic AD lesions and correlates with the magnitude of the Th2 signals.⁵ While various different T-cell pathways have been targeted in clinical trials of AD, the functional effects of the inflammatory pathways on skin keratinocytes have largely been ignored.^{6,7}

Alongside the immune skin infiltrate, spongiosis and keratinocyte hyperplasia are the cardinal features of epidermal changes in AD. In addition to the gene mutation-mediated reduction of filaggrin expression, type 2 inflammation also reduces keratinocyte filaggrin expression, thereby further damaging the skin barrier.^{8,9} Importantly, beyond their role in maintaining the physical barrier of the skin, keratinocytes also act as innate immune sentinels, and express pattern-recognition receptors, ligation of which regulates keratinocyte synthesis of cytokines, antimicrobial peptides (AMPs) and antigen presentation to immune cells.^{10–16}

The role of IL-17 and IL-22 cytokines in regulating AMPs such as S100 proteins and β -defensins is well established^{17–22} and the importance of these pathways in psoriasis has been validated by clinical demonstration of the effectiveness of inhibitory monoclonal antibody therapy;^{23,24} however, their precise function in AD is less clear. To study the key pathways driving AD, where targeted intervention may prove most fruitful, direct quantitation of the immune signals (e.g. cytokines) can be undertaken. However, as molecular quantitation of the cytokine transcripts does not predict the importance of a specific pathway in AD, it is necessary to study the outcome of the epidermal responses to different inflammatory stimuli to properly define their role. Thus, to characterize the keratinocyte immunophenotype it is necessary to be able to investigate the skin transcriptome to a cellular resolution. Single-cell analysis can offer an approach to this question but is limited by the technical challenge of achieving adequate encapsulation of enough cells of interest with minimal transcriptomic disturbance. Here we show that it is possible to employ machine learning to resolve the keratinocyte transcriptomic signal from the nonkeratinocyte skin transcriptome, revealing important insights into the pathogenesis of AD.

Methods

Microarray data analysis

Microarray datasets were obtained from the Gene Expression Omnibus (GEO, National Center for Biotechnology Information) and were analysed from raw data in R and normalized

according to platform specifics. For Affymetrix microarray platforms, classic microarray quality control was performed using the Bioconductor `arrayQualityMetrics` tool and were normalized to obtain expression values by Gene Chip Robust Multiarray Averaging (GCRMA) methods within the Affymetrix package. Illumina platforms and other technologies were quantile normalized using the `lumi` or `limma` Bioconductor packages (<http://bioconductor.org/>).

Unsupervised network clustering

The inflammatory skin disease datasets GSE32924, GSE36842 and GSE34248 were processed as above and subsequently merged and batch corrected using the COMBAT tool within the SVA Bioconductor package (<http://bioconductor.org/>). Differential gene expression analysis between healthy controls and lesional skin, within disease lesional and nonlesional, and across disease lesional comparisons was conducted using a filtering of Benjamini–Hochberg adjusted P -value > 0.05 , log (2)-fold difference $\times 1$ using the `limma` Bioconductor package. The expression values of 4620 probset-IDs, corresponding to 3066 unique genes were input into MIRU (now, GraphiaPro) for network analysis.^{25,26} A transcript-to-transcript correlation matrix using Pearson correlation coefficient of $r \geq 0.7$ was created, which best defined the clusters by granularity, biological meaning and significance of gene annotation (Data S1; see Supporting Information). The resulting network graph was then clustered into groups of genes using the Markov Clustering algorithm (MCL) at an inflation value of 3.1 and minimum cluster size of 10 genes, giving 50 clusters. The gene list for each cluster was interrogated for gene ontology using the web-based analysis tool ToppFun within the ToppGene suite.²⁷ The REVIGO online tool was used to provide a single biological process term for each cell-based cluster, selecting that with both the lowest Benjamini–Hochberg P -value and a term dispensability of zero.²⁸ The full annotation for the 50 clusters is available in Data S2 (see Supporting Information).

Reference cutaneous cell populations datasets

To curate cell profiles for input as CIBERSORT reference signatures, we collated seven datasets from GEO: GSE36287 [keratinocytes stimulated with interferon (IFN)- α , IFN- γ , IL-13, IL-17A, IL-4, tumour necrosis factor (TNF)- α and an unstimulated control], GSE7216 [keratinocytes stimulated with IL-1 β , IL-22, IL-26 and keratinocyte growth factor (KGF)], GSE34308 (dermal fibroblasts), GSE74158 (skin-resident CD4, CD8 and regulatory T cells), GSE4570 (melanocytes), GSE49475 (activated Langerhans cells and CD11c⁺ dermal dendritic cells) and GSE23618 (steady-state Langerhans cells). Datasets were normalized separately, and gene expression of sample replicates averaged by mean before combining into a single file for upload to CIBERSORT as a signature genes matrix (Table S1; see Supporting Information). Gene replicates are discounted by CIBERSORT in favour of the gene with the highest mean expression across the samples.

Bulk skin datasets

Eleven datasets of skin biopsies from inflammatory skin diseases at baseline and under treatment conditions were obtained from GEO: GSE11903,^{29,30} GSE120721,³¹ GSE120899,³² GSE130588,⁴ GSE133385,³³ GSE32924,³ GSE34248,³⁴ GSE36842,⁵ GSE58558,³⁵ GSE59294³⁶ and GSE99802³⁷ (full description is available in Methods S1 and Figures S1 and S2; see Supporting Information).

Running CIBERSORT

To deconvolute the bulk data we used CIBERSORT, a machine-learning linear support vector regression algorithm.³⁸ Optimization of the CIBERSORT tool for deconvolution of skin is described in Methods S1 (see Supporting Information). Datasets of bulk skin samples were deconvoluted against the reference signature sets using the online version of the CIBERSORT algorithm. Reference signature files were provided as the *signature gene file*, while normalized expression data of bulk samples were provided as the *mixture file*. All run settings were kept at default. The output provided by CIBERSORT was downloaded as a .txt file, where the relative abundance of each cellular signature was normalized as a per cent of sample.

Results

Gene co-expression analysis of inflammatory skin disease genes reveals immune and keratinocyte involvement

Firstly, we set out to examine the lesional signals from skin biopsies of AD and psoriasis by comparing lesional against nonlesional transcriptomes (AD-Les, AD-Non, Ps-Les, Ps-Non, respectively). In line with previous reports,^{3,5,34} unsupervised differential expression analysis identified 3066 genes. Transcript-to-transcript clustering (GraphiaPro, Pearson $r \geq 0.7$, MCL = 3.1, > 10 clustered genes) identified 50 clusters (Figure 1a). Annotation revealed three clusters (11, 14 and 28) encoding immune-related processes such as lymphocyte activation, IFN and cytokine signalling (Figure 1b–d; Data S2; see Supporting Information). The relative expression pattern across these clusters showed similar changes in lesions, regardless of disease, and the least expression in healthy skin. Interestingly, AD nonlesional skin showed a prominent defence response (cluster 28), suggesting a subclinical immune alteration in nonlesional AD skin compared with healthy skin.^{3,39,40}

Strikingly, clusters 1, 6, 9 and 18 (Figure 1e–h and Data S2; see Supporting Information) were enriched in biological processes characteristic for keratinocytes. Genes in clusters 1 and 18 were most highly expressed in healthy tissue and represented processes of epidermis development and skin development, respectively, suggesting aberrant regulation of these processes in inflammatory skin disease. In contrast, genes in cluster 9 showed strong correlation with the expression of immune-mediated inflammation genes, which suggests that the association may be causal. Cluster-to-cluster gene expression by

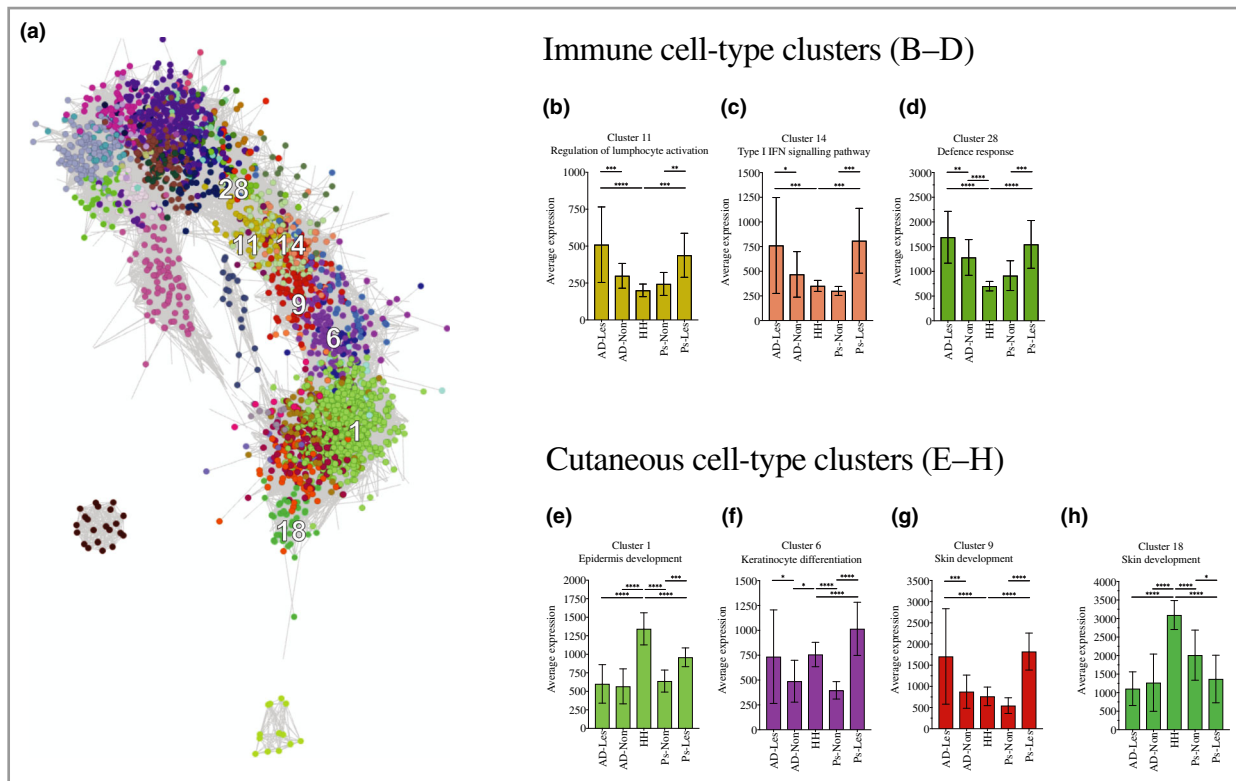


Figure 1 Unsupervised co-expression analysis of whole skin from healthy, atopic and psoriatic skin. (a) Transcript-to-transcript clustering of 4620 differentially expressed genes of AD-Les, AD-Non, Ps-Les and Ps-Non skin conditions compared with HH (false discovery rate: P -value < 0.05 , log fold-change $< -2 / > 2$). Gene-to-gene co-expression correlation of Pearson $r \geq 0.7$ was retained for Markov clustering algorithm using an inflation value of 3.1. (b–h) The top 50 clusters were annotated for biological process, of which seven clusters were identified as cell based. The average expression of all the genes in the cluster is shown per phenotype. Normality testing performed using the D’Agostino–Pearson method indicated the use of nonparametric Kruskal–Wallis ANOVA with multiple comparison performed to test the significance of AD and Ps-Les against Ps-Non, and HH against AD and Ps-Les and Ps-Non: * $P < 0.05$, ** $P < 0.01$, *** $P < 0.001$, **** $P < 0.0001$. Error bars show median \pm 95% confidence interval. IFN, interferon; AD, atopic dermatitis; AD-Les, AD lesional; AD-Non, AD nonlesional; HH, healthy control; Ps-Les, psoriasis lesional; Ps-Non, psoriasis nonlesional.

tissue showed high correlation [Pearson correlation ≥ 0.7 (data not shown)]. It is notable that genes in cluster 9 include *KRT6A/B* and *KRT16*, and the *S100* and *SERPIN* encoding proteins which are known to be involved in epidermal perturbation from inflammation and hyperproliferative barrier breach,^{2,41,42} indicating that the crosstalk between immune inflammation and keratinocyte function is important for lesion pathogenesis.

Resolution of whole-skin samples into constituent cellular profiles

We trained a machine-learning algorithm, CIBERSORT, to resolve from bulk expression data the transcriptomic signatures of keratinocyte responses. Firstly, we trained CIBERSORT to resolve gene expression profiles of purified cellular populations and tested this on whole-tissue transcriptomic data from split skin³¹ (epidermis and dermis) to identify the relative proportion of cells. We then utilized laser-captured dermal and epidermal regions from both healthy and AD skin to demonstrate that the algorithm could reliably separate relative proportions of the keratinocyte and fibroblast composition of whole skin in

uninflamed and inflamed settings (Figure 2a, b and Table S2; see Supporting Information). We expanded this approach by utilizing a training set of transcriptomes for melanocytes, resident regulatory CD4 and CD8 T cells, steady-state and activated Langerhans cells, and CD11c⁺ dermal dendritic cells to increase the resolution of the cellular skin components (Figure 2c and Table S3; see Supporting Information).

Deconvolution reveals a prevalence of keratinocyte 2 and progression of keratinocyte 17 immunophenotypes during the course of the inflammation in atopic dermatitis

To identify subpopulations of keratinocytes showing a molecular response to a specific inflammatory cytokine, we further trained the algorithm to resolve keratinocytes responding to IFN- α and IFN- γ [keratinocyte (KC)1], IL-4 and IL-13 (KC2), IL-17A (KC17), KGF, IL-26, IL-22, TNF, IL-1 β , as well as resting (Figure 3 and Figure S3; see Supporting Information). These were tracked across 14 healthy controls, 18 AD-Non, seven AD acute lesional skin samples (AD-AcL) and 18 AD chronic lesional samples (AD-ChL) (GSE32924 and GSE36842) and 14 Ps-Non

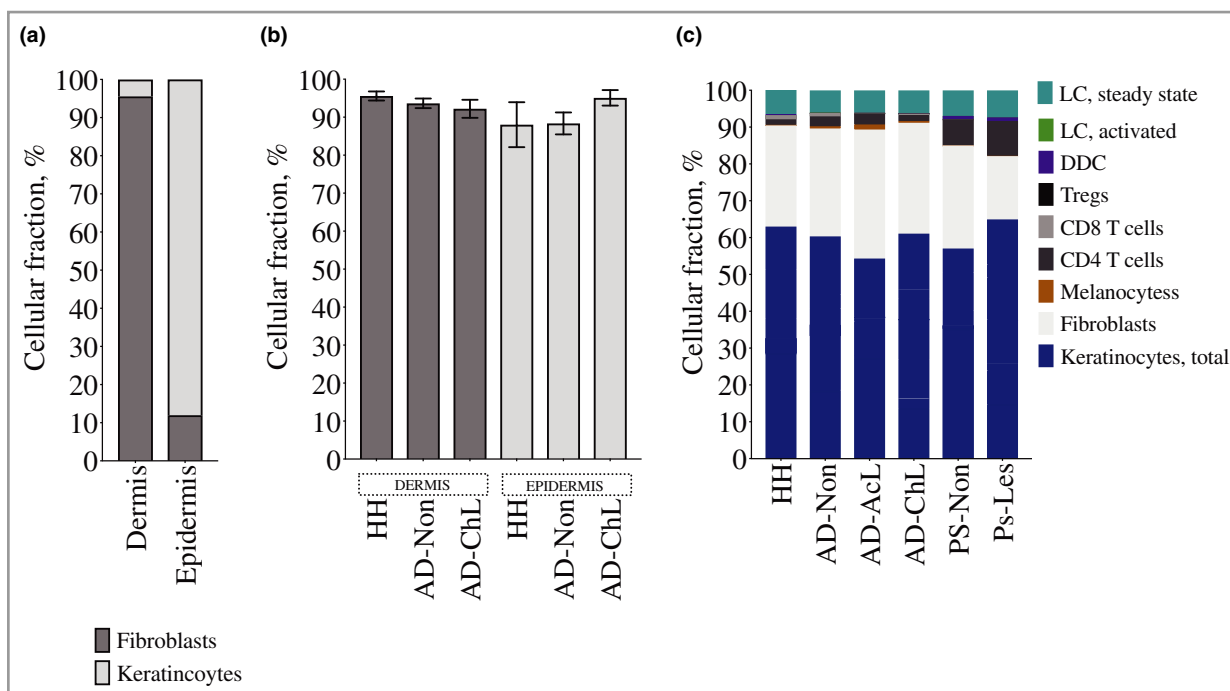


Figure 2 Machine-learning resolution of whole-skin samples into constituent cellular profiles. (a) Identification of key cellular signatures (fibroblasts, dark grey; keratinocytes, light grey) in microdissected samples from dermis and epidermis by machine learning (healthy dermis, $n = 6$; healthy epidermis, $n = 10$). (b) Inflammation/disease status (HH, AD-Non, AD-ChL) of dermis or epidermis does not affect the correct deconvolution of cellular components within the bulk disease tissue. Dermis: HH, $n = 6$; AD-Non, $n = 5$; AD-ChL, $n = 5$. Epidermis: HH, $n = 10$; AD-Non, $n = 5$; AD-ChL, $n = 5$. (a, b) Default CIBERSORT settings: 100 permutations, $\kappa = 999$, q -value = 0.3, number of barcode genes 50–150. Training signatures: GSE36287, unstimulated keratinocytes; GSE34308, skin fibroblasts (Table S2; see Supporting Information). (c) Whole skin from HH, patients with AD (AD-Non, AD-AcL and AD-ChL, respectively) and patients with psoriasis (Ps-Non and Ps-Les, respectively) resolved into relative fractions of cutaneous cell populations of nine transcriptomic signatures: keratinocytes; fibroblasts; melanocytes; $CD4^+$, $CD8^+$ and regulatory T cells (Tregs); dermal dendritic cells (DDCs); and, steady-state and activated Langerhans cells (LCs). The mean percentage of each of the signatures is shown relative to the remaining signatures. HH ($n = 14$), patients with AD (AD-Non, $n = 18$; AD-AcL, $n = 7$; AD-ChL, $n = 18$) and patients with psoriasis (Ps-Non, $n = 14$; Ps-Les, $n = 14$). Default CIBERSORT settings and training signatures are shown in Table S3 (see Supporting Information). AD, atopic dermatitis; AD-AcL, AD acute lesional sample; AD-ChL, AD chronic lesional sample; AD-Les, AD lesional sample; AD-Non, AD nonlesional sample; HH, healthy controls; Ps-Les, psoriasis lesional sample; Ps-Non, psoriasis nonlesional sample.

samples and 14 in Ps-Les samples to investigate disease-related shift in the transcriptomic programme of these cells (Figure 3b–e). As expected in AD, a strong KC2 signal was clearly detectable, showing that keratinocytes in chronic lesions were responding to type 2 cytokines in comparison with healthy skin (Figure 3c). Interestingly, this signal was equally strong in nonlesional skin suggesting that this dysregulation may be systemic in AD.

A keratinocyte IFN programme, KC1, was prominent in Ps-Les and absent from Ps-Non samples (Bonferroni $P < 0.001$) (Figure 3b). KC1 was also found in chronic lesions from AD samples, showing a trend of increase from nonlesional (Bonferroni $P = 0.0048$) and acute lesional stages [Figure 3b and Figure S4 (see Supporting information) for GSE133385³³], inferring the complex Th2/Th17/Th1 inflammation experienced by the epidermis of chronic AD lesions also alters the transcriptomic programme of keratinocytes. As expected, the KC17 signal was significantly elevated in psoriatic lesions compared with healthy controls and paired nonlesional samples (Bonferroni $P < 0.001$) (Figure 3d). AD keratinocytes showed

an IL-17 sensing signal in lesional as well as nonlesional skin but was only suggestive of an intensification of this process in chronic lesions (Bonferroni $P = 0.0555$) (Figure 3d). KC17 appeared to dominate in chronic AD lesions, suggesting an evolution in Th17 pathway over time.

Treatment-specific modification of keratinocyte immunophenotype signature

Microarray data from patients with psoriasis treated with etanercept showed that KC2 was neither lesion nor treatment defining (Figure 4a), but longitudinal abrogation of KC17 ($P < 0.0001$) underscored the role of this pathway in psoriasis pathogenesis (Figure 4b). The immunophenotypic signature of response to AD treatment was more nuanced. Khattri *et al.* showed that ciclosporin administration reduced AD-related keratinocyte products and is linked to specific T-cell subsets and their cytokines.³⁵ Despite efficacy and improvement in disease severity scores across the cohort

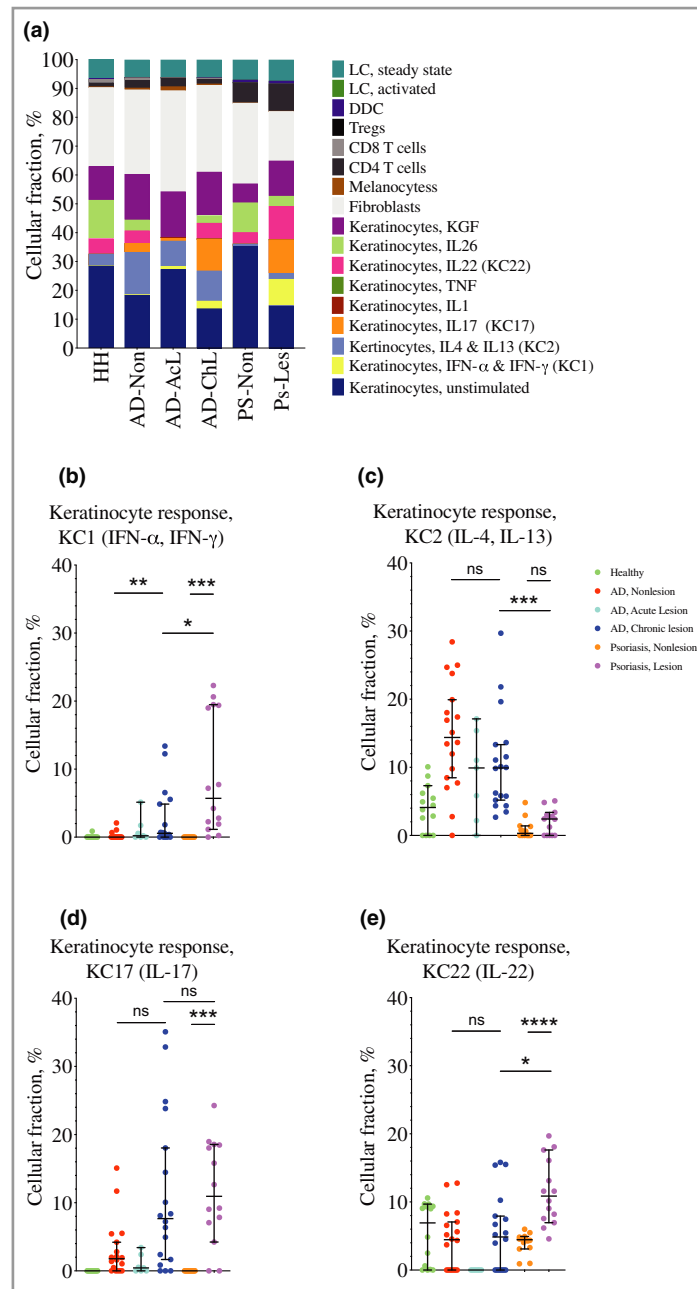


Figure 3 Resolution of whole-skin samples into constituent cellular profiles using machine learning. (a) Deconvolution of keratinocyte signature into profiles representing keratinocyte immunophenotypes across the six skin conditions: healthy (HH), AD nonlesional (AD-Non), AD acute lesional (AD-AcL), AD chronic lesional (AD-ChL), psoriasis nonlesional (Ps-Non), psoriasis lesional (Ps-Les). [Default CIBERSORT settings, training signatures: keratinocytes (unstimulated, stimulated with IFN- α , IFN- γ , IL-17, IL-1 β , TNF, IL-22, IL-26, KGF); fibroblasts; melanocytes; CD4+, CD8 + and regulatory T cells (Tregs); dermal dendritic cells (DDCs); and, steady-state and activated Langerhans cells (LCs) here, Table S1; see Supporting Information]. (b–e) Individual keratinocyte immunophenotypes; (b) KC1 (response to IFN- α , IFN- γ); (c) KC2 (response to IL-4, IL-13); (d) KC17 (response to IL-17), (e) KC22 (response to IL-22); remaining keratinocyte fractions shown in Figure S3 (see Supporting Information). Healthy patients ($n = 14$, green), AD-Non patients ($n = 18$, red), AD-AcL patients ($n = 7$, cyan), AD-ChL patients ($n = 18$, blue), Ps-Non patients ($n = 14$, orange) and Ps-Les patients ($n = 14$, magenta). Normality testing performed by D’Agostino–Pearson method showed a normal distribution for KC22 samples. Unpaired nonparametric Mann–Whitney tests for non-normal data and unpaired t-test for normally distributed data, Bonferroni corrected for multiple testing: * $P < 0.05$, ** $P < 0.01$, *** $P < 0.001$, **** $P < 0.0001$. Error bars show median \pm 95% confidence interval. IFN, interferon; IL, interleukin; KC, keratinocyte; KGF, keratinocyte growth factor; TNF, tumour necrosis factor.

(50% improvement in baseline SCORing AD index, SCORAD50),³⁵ ciclosporin treatment did not reduce the KC2 fraction in either nonlesional or lesional samples (Figure 4c).

However, the KC17 fraction in lesional keratinocytes was significantly reduced by ciclosporin ($P = 0.0085$) which was depleted to a nonlesional skin phenotype (Figure 4d). Our

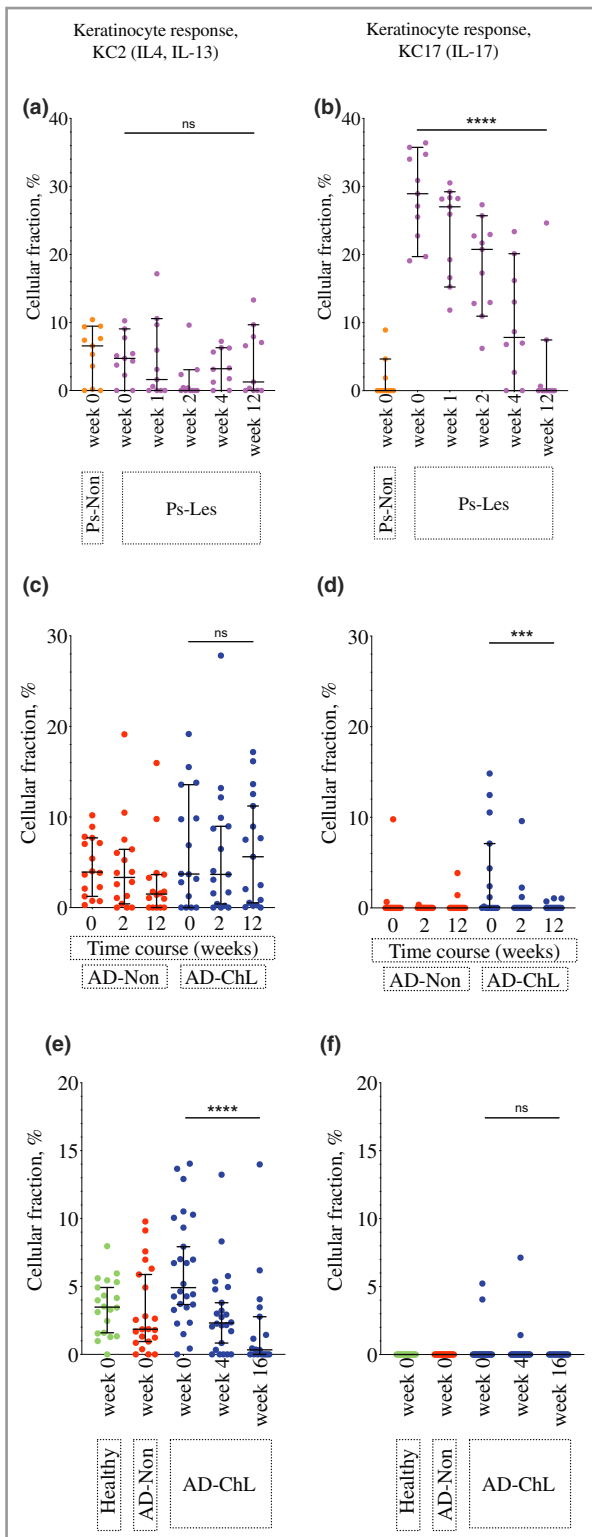


Figure 4 Response of disease-related keratinocyte fractions, KC2 and KC17, to treatment of psoriasis and AD. (a, b) KC2 (a) and KC17 (b) in whole skin from patients with psoriasis undergoing etanercept treatment [nonlesional (week 0 only, $n = 11$, orange) and lesional (weeks 0, 1, 2, and 12, $n = 11$; week 4, $n = 10$, magenta)]. [GSE11903 (Default CIBERSORT settings and training signatures: as in Figure 3 and Table S1; see Supporting Information)]. (c, d) KC2 (c) and KC17 (d) during a time course of ciclosporin treatment at baseline [AD-Non (red), $n = 16$; AD-ChL (blue), $n = 16$], mid-treatment (2 weeks) (AD-Non, $n = 17$; AD-ChL, $n = 16$) and end of treatment at 12 weeks (AD-Non, $n = 17$; AD-ChL, $n = 16$). [GSE58558 (Default CIBERSORT settings, training signatures: as in Figure 3 and Table S1; see Supporting Information)]. (e, f) KC2 (e) and KC17 (f) fractions in healthy (green), AD-Non (red) and AD-ChL (blue) AD samples during a time course of dupilumab treatment at baseline (HH, $n = 20$; AD-Non, $n = 42$; AD-ChL, $n = 51$), mid-treatment (4 weeks) (AD-ChL, dupilumab-treated $n = 24$) and end of treatment (16 weeks) (AD-ChL, dupilumab-treated $n = 18$). [GSE130588 (Default CIBERSORT settings, training signatures: as in Figure 3 and Table S1; see Supporting Information)]. Normality testing performed by the D'Agostino–Pearson method indicated using nonparametric Kruskal–Wallis ANOVA with multiple comparison performed (Dunn's method) to test the significance of baseline to end of treatment in lesions: * $p < 0.05$, ** $p < 0.01$, *** $p < 0.001$, **** $p < 0.0001$. Error bars show median \pm 95% confidence interval. AD, atopic dermatitis; AD-ChL, AD chronic lesional; AD-Non, AD-nonlesional; HH, healthy controls; KC, keratinocyte; ns, not significant.

To follow the effect of anti-Th2 treatment on keratinocyte transcriptomic responses, we considered two skin microarray datasets under dupilumab treatment.^{4,36} The earlier dataset³⁶ showed dose dependency of dupilumab treatment in AD, and we confirmed this response in the KC2 immunophenotype (Figure S6; see Supporting Information). We used the GEO microarray dataset GSE130588, where bulk skin microarray data was obtained from patients with AD treated with a higher dose (400 mg) of dupilumab with biopsies taken at treatment initiation, 4 weeks and 16 weeks on the conclusion of treatment, along with a healthy control cohort. Biopsies were taken from the same lesional site and showed a clinical and transcriptomic improvement in clinical atopy with treatment in established, ongoing lesions. Interestingly, very few of the AD samples, including many of the lesional biopsies, showed a KC17 fraction. Dupilumab treatment demonstrated a dramatic early reduction in the KC2 fraction of lesions at 4 weeks compared with baseline, which was sustained at 16 weeks ($P < 0.0001$) (Figure 4e). At the start of treatment, AD lesions had an increased KC2 profile compared with healthy controls, which resolved to be comparable by the end of anti-IL-4, IL-13 treatment.

Finally, the IL-22-stimulated keratinocyte signature (KC22) included in our CIBERSORT deconvolution panel was not upregulated in AD (Figure 3e). However, when testing the response of this KC22 fraction on anti-IL-22 treatment using the public dataset GSE99802,³⁷ we found a corresponding reduction in the KC22 signal (Figure S7; see Supporting Information).

further analysis of the apremilast treatment in the AD dataset shows KC2 to be high at baseline and significantly responsive to treatment, complementing the findings of the original study reporting a decrease in Th2 cytokines in AD lesions³² (Figure S5; see Supporting Information).

Discussion

Despite our understanding of the role of inflammatory cells in AD, and identification of the different inflammatory signals evident in AD, it is surprising that little attention has been paid to characterizing the keratinocyte response in detail. This has perhaps, in part, been due to technical challenges associated with addressing the question. Standard approaches to bioinformatic analysis of transcriptomic studies of AD⁴ employ statistical tools to identify differentially expressed genes in lesions vs. nonlesions and can utilize gene-set enrichment analysis based on the functional annotation of the differentially expressed transcripts to identify cellular processes that are more or less prominent in AD.

However, such a macro view of the AD transcriptome prevents characterization of individual responses of the various cell types comprising skin. Widely used approaches to look at individual cell populations include flow cytometry and immunohistochemistry. Despite the routine application of these methodologies, and valuable insights they can provide for a relatively narrow set of markers, they inform analysis of cell phenotype in only a relatively limited way, partly because both of these techniques require a monoclonal antibody label of which a limited panel can be applied to a single sample. Single-cell sequencing from whole skin or from flow-sorted populations would allow the investigator to undertake detailed characterization of cell types in AD in a nonhypothesis-driven manner. However, as yet, these approaches are limited by cost, and the relatively low number of sequenced cells as a proportion of the whole-tissue sample may present a sampling bias. We sought to address cellular analysis within tissue by a different approach. Using machine learning on published datasets, we trained an algorithm to identify different skin-cell types and then cellular responses to different inflammatory responses of interest. We tested this algorithm on transcriptomic studies of microdissected healthy skin and psoriatic skin that has a known immune pathway dependence, showing that our approach is a powerful method for investigating transcriptomic signatures in skin samples of complex disease.

Applying machine-learning-based analysis to existing datasets of AD disease stages and during treatment has confirmed the constitutive atopic skin phenotype in patients with AD. An altered transcriptomic programme in keratinocytes was evident in all samples (lesional and nonlesional) which reflected Th2 sensing by keratinocytes that we termed 'KC2', and similar findings have been reported by others.^{3,5} Further, we show the immunophenotype shift characteristic of lesion progression modifies keratinocyte profiles to an IL-17 (KC17) and IFN (KC1) sensing phenotype. Thus, we could demonstrate that although acute AD lesions show a strong Th2 signal, and chronic lesions have Th1 and Th17 signals, the Th2-related process is amplified rather than a switch away from a type 2 cytokine response in chronic lesions.

Effective treatment of psoriasis with etanercept showed a reversal of the dominant KC17 profile of lesional skin to that of unaffected skin. However, in AD, remarkably, and despite

resolution of skin inflammation as measured by disease severity, ciclosporin did not modify the KC2 profile of lesional skin. Instead, AD disease remission with ciclosporin correlated with loss of the KC17 signal. In contrast to this, with dupilumab, there is a striking loss of the KC2 signal associated with disease remission, but the previously observed KC17 response was not found in these samples (Figure 4f). This underscores the critical role of type 2 cytokines in AD and might suggest a strong role for the IL-17 pathway in AD pathogenesis; it might also reflect the complex immunophenotype of the disease and potential immune mediator redundancy.

Our analysis to computationally resolve keratinocyte subpopulations by their sensing of immune-related signals does not address AD as a disease driven by epidermal disruption or systemic immune abnormalities. Indeed, we see evidence of some individual variation at a keratinocyte level, particularly of KC2 and KC17 immunophenotypes. It is important to note that our analysis derives from adult biopsy data, and paediatric cutaneous inflammation, especially relevant for AD, may alter these immunophenotypes. We postulate that various environmental factors, such as commensal dysbiosis, may contribute to individual variation in epidermal sensing by keratinocytes and may regulate the epidermal response, both modifying and modified by immune infiltrate signals. This theory would suggest that perturbation of the immune signal alone may, in some situations, be insufficient to resolve the keratinocyte immunophenotype. Furthermore, such considerations emphasize the importance of characterizing the epidermal responses alongside the immune signals in molecular studies of AD.

In summary, *in silico* deconvolution of the transcriptional phenotype of AD keratinocytes has revealed two levels of pathology. Firstly, individuals with AD epidermis demonstrate keratinocyte sensing of type 2 cytokines. Secondly, although the IL-4/IL-13 signal becomes enhanced in chronic AD lesions, it appears that induction of an IL-17 response acts as a key switch between acute and chronic AD. This confirms the model of sequential activation of Th cell responses across the development and chronicity of cutaneous lesions. Finally, we showed that despite disease resolution with both ciclosporin and dupilumab, ciclosporin treatment rebalances the KC17 subpopulation comparable to normal skin but does not modify type 2 cytokine sensing, whereas, dupilumab therapy reverses the KC2 dominance in lesional AD. Taken together, these observations suggest that while type 2 cytokines appear to drive AD biology, the efficacy of ciclosporin in AD is likely to lie beyond the targeting of T cells with resultant Th17 inhibition and that other pathways modified by this effective therapy should be explored as potential therapeutic targets.

Acknowledgments

We thank our funding bodies, the MRC and Wellcome Trust, and the iCASE PhD studentship sponsor, Unilever, for providing the resources to undertake this research. We also thank Rebecca Ginger, formerly of Unilever (Colworth Park, UK) for previous discussions and contributions.

References

- 1 Biedermann T, Skabytska Y, Kaesler S, Volz T. Regulation of T cell immunity in atopic dermatitis by microbes: the yin and yang of cutaneous inflammation. *Front Immunol* 2015; **6**:353.
- 2 Ungar B, Garcet S, Gonzalez J *et al.* An integrated model of atopic dermatitis biomarkers highlights the systemic nature of the disease. *J Invest Dermatol* 2017; **137**:603–13.
- 3 Suárez-Fariñas M, Tintle SJ, Shemer A *et al.* Nonlesional atopic dermatitis skin is characterized by broad terminal differentiation defects and variable immune abnormalities. *J Allergy Clin Immunol* 2011; **127**:954–64.e1–4.
- 4 Guttman-Yassky E, Bissonnette R, Ungar B *et al.* Dupilumab progressively improves systemic and cutaneous abnormalities in patients with atopic dermatitis. *J Allergy Clin Immunol* 2019; **143**:155–72.
- 5 Gittler JK, Shemer A, Suárez-Fariñas M *et al.* Progressive activation of T(H)2/T(H)22 cytokines and selective epidermal proteins characterizes acute and chronic atopic dermatitis. *J Allergy Clin Immunol* 2012; **130**:1344–54.
- 6 Mansouri Y, Guttman-Yassky E. Immune pathways in atopic dermatitis, and definition of biomarkers through broad and targeted therapeutics. *J Clin Med* 2015; **4**:858–73.
- 7 Ariëns LFM, Gadkari A, van Os-Medendorp H *et al.* Dupilumab versus cyclosporine for the treatment of moderate-to-severe atopic dermatitis in adults: indirect comparison using the Eczema Area and Severity Index. *Acta Derm Venereol* 2019; **99**:851–7.
- 8 Brunner PM, Guttman-Yassky E, Leung DYM. The immunology of atopic dermatitis and its reversibility with broad-spectrum and targeted therapies. *J Allergy Clin Immunol* 2017; **139**:S65–76.
- 9 Hönzke S, Wallmeyer L, Ostrowski A *et al.* Influence of Th2 cytokines on the cornified envelope, tight junction proteins, and β -defensins in filaggrin-deficient skin equivalents. *J Invest Dermatol* 2016; **136**:631–9.
- 10 Nestle FO, Di Meglio P, Qin J-Z, Nickoloff BJ. Skin immune sentinels in health and disease. *Nat Rev Immunol* 2009; **9**:679–91.
- 11 Pfalzgraff A, Brandenburg K, Weindl G. Antimicrobial peptides and their therapeutic potential for bacterial skin infections and wounds. *Front Pharmacol* 2018; **9**:281.
- 12 Colombo I, Sangiovanni E, Maggio R *et al.* HaCaT cells as a reliable *in vitro* differentiation model to dissect the inflammatory/repair response of human keratinocytes. *Mediators Inflamm* 2017; **2017**:1–12.
- 13 Nakagawa S, Matsumoto M, Katayama Y *et al.* *Staphylococcus aureus* virulent PSM α peptides induce keratinocyte alarmin release to orchestrate IL-17-dependent skin inflammation. *Cell Host Microbe* 2017; **22**:667–77.e5.
- 14 Lai Y, Gallo RL. AMPed up immunity: how antimicrobial peptides have multiple roles in immune defense. *Trends Immunol* 2009; **30**:131–41.
- 15 Selsted ME, Ouellette AJ. Mammalian defensins in the antimicrobial immune response. *Nat Immunol* 2005; **6**:551–7.
- 16 Nickoloff BJ, Turka LA. Immunological functions of non-professional antigen-presenting cells: new insights from studies of T-cell interactions with keratinocytes. *Immunol Today* 1994; **15**:464–9.
- 17 Valeri M, Raffatelli M. Cytokines IL-17 and IL-22 in the host response to infection. *Pathog Dis* 2016; **74**:ftw111.
- 18 Archer NK, Adappa ND, Palmer JN *et al.* Interleukin-17A (IL-17A) and IL-17F are critical for antimicrobial peptide production and clearance of *Staphylococcus aureus* nasal colonization. *Infect Immun* 2016; **84**:3575–83.
- 19 Dixon BREA, Radin JN, Piazuelo MB *et al.* IL-17a and IL-22 induce expression of antimicrobials in gastrointestinal epithelial cells and may contribute to epithelial cell defense against *Helicobacter pylori*. *PLoS One* 2016; **11**:e0148514.
- 20 Yano S, Banno T, Walsh R, Blumenberg M. Transcriptional responses of human epidermal keratinocytes to cytokine interleukin-1. *J Cell Physiol* 2008; **214**:1–13.
- 21 Sa SM, Valdez PA, Wu J *et al.* The effects of IL-20 subfamily cytokines on reconstituted human epidermis suggest potential roles in cutaneous innate defense and pathogenic adaptive immunity in psoriasis. *J Immunol* 2007; **178**:2229–40.
- 22 Guilloteau K, Paris I, Pedretti N *et al.* Skin inflammation induced by the synergistic action of IL-17A, IL-22, oncostatin M, IL-1 α , and TNF- α recapitulates some features of psoriasis. *J Immunol* 2010; **184**:5263–70.
- 23 Guttman-Yassky E, Lowes MA, Fuentes-Duculan J *et al.* Low expression of the IL-23/Th17 pathway in atopic dermatitis compared to psoriasis. *J Immunol* 2008; **181**:7420–7.
- 24 Guttman-Yassky E, Krueger JG. Atopic dermatitis and psoriasis: two different immune diseases or one spectrum? *Curr Opin Immunol* 2017; **48**:68–73.
- 25 Freeman TC, Goldovsky L, Brosch M *et al.* Construction, visualization, and clustering of transcription networks from microarray expression data. *PLoS Comput Biol* 2007; **3**:2032–42.
- 26 Theocharidis A, van Dongen S, Enright AJ, Freeman TC. Network visualization and analysis of gene expression data using BioLayout Express(3D). *Nat Protoc* 2009; **4**:1535–50.
- 27 Chen J, Bardes EE, Aronow BJ, Jegga AG. ToppGene suite for gene list enrichment analysis and candidate gene prioritization. *Nucleic Acids Res* 2009; **37**:W305–11.
- 28 Supek F, Bošnjak M, Škunca N, Šmuc T. REVIGO summarizes and visualizes long lists of gene ontology terms. *PLoS One* 2011; **6**:e21800.
- 29 Zaba LC, Suárez-Fariñas M, Fuentes-Duculan J *et al.* Effective treatment of psoriasis with etanercept is linked to suppression of IL-17 signaling, not immediate response TNF genes. *J Allergy Clin Immunol* 2009; **124**:1022–30.e395.
- 30 Correa da Rosa J, Kim J, Tian S *et al.* Shrinking the psoriasis assessment gap: early gene-expression profiling accurately predicts response to long-term treatment. *J Invest Dermatol* 2017; **137**:305–12.
- 31 Esaki H, Ewald DA, Ungar B *et al.* Identification of novel immune and barrier genes in atopic dermatitis by means of laser capture microdissection. *J Allergy Clin Immunol* 2015; **135**:153–63.
- 32 Simpson EL, Imafuku S, Poulin Y *et al.* A phase 2 randomized trial of apremilast in patients with atopic dermatitis. *J Invest Dermatol* 2019; **139**:1063–72.
- 33 Pavel AB, Song T, Kim HJ *et al.* Oral janus kinase/SYK inhibition (ASN002) suppresses inflammation and improves epidermal barrier markers in patients with atopic dermatitis. *J Allergy Clin Immunol* 2019; **144**:1011–24.
- 34 Bigler J, Rand HA, Kerkof K *et al.* Cross-study homogeneity of psoriasis gene expression in skin across a large expression range. *PLoS One* 2013; **8**:e52242.
- 35 Khattri S, Shemer A, Rozenblit M *et al.* Cyclosporine in patients with atopic dermatitis modulates activated inflammatory pathways and reverses epidermal pathology. *J Allergy Clin Immunol* 2014; **133**:1626–34.
- 36 Hamilton JD, Suárez-Fariñas M, Dhingra N *et al.* Dupilumab improves the molecular signature in skin of patients with moderate-to-severe atopic dermatitis. *J Allergy Clin Immunol* 2014; **134**:1293–300.
- 37 Brunner PM, Pavel AB, Khattri S *et al.* Baseline IL-22 expression in patients with atopic dermatitis stratifies tissue responses to fezakinumab. *J Allergy Clin Immunol* 2019; **143**:142–54.
- 38 Newman AM, Liu CL, Green MR *et al.* Robust enumeration of cell subsets from tissue expression profiles. *Nat Methods* 2015; **12**:453–7.

- 39 Brunner PM, Emerson RO, Tipton C *et al.* Nonlesional atopic dermatitis skin shares similar T-cell clones with lesional tissues. *Allergy* 2017; **72**:2017–25.
- 40 Tang TS, Bieber T, Williams HC. Are the concepts of induction of remission and treatment of subclinical inflammation in atopic dermatitis clinically useful? *J Allergy Clin Immunol* 2014; **133**:1615–25.e1.
- 41 Lessard JC, Piña-Paz S, Rotty JD *et al.* Keratin 16 regulates innate immunity in response to epidermal barrier breach. *Proc Natl Acad Sci U S A* 2013; **110**:19537–42.
- 42 Rorke EA, Adhikary G, Young CA *et al.* Structural and biochemical changes underlying a keratoderma-like phenotype in mice lacking suprabasal AP1 transcription factor function. *Cell Death Dis* 2015; **6**: e1647.

Supporting Information

Additional Supporting Information may be found in the online version of this article at the publisher's website:

Summary S1 Methods S1, Legends for Data S1, S2, Figures S1–S7 and Tables S1–S3.

Methods S1 Optimizing CIBERSORT for deconvolution of bulk skin.

Data S1 Biological process annotation of cell-based clusters from Figure 1.

Data S2 Co-expression clusters from Figure 1 (50 clusters).

Figure S1 Testing the stability of the CIBERSORT algorithm.

Figure S2 Determining the fidelity of the CIBERSORT algorithm.

Figure S3 Resolution of whole skin samples into constituent cellular profiles using machine learning.

Figure S4 Response of interferon (IFN)- α , IFN- γ -stimulated keratinocyte fraction to JK/SYK inhibition.

Figure S5 Response of interleukin (IL)-4, IL-13-stimulated keratinocyte fraction to apremilast treatment.

Figure S6 Dose-dependent response of interleukin (IL)-4, IL-13-stimulated keratinocyte fraction to dupilumab treatment.

Figure S7 Response of interleukin (IL)-22-stimulated keratinocyte fraction to fezakinumab treatment.

Table S1 Training samples of keratinocytes, skin dermal fibroblasts and others.

Table S2 Training samples of unstimulated keratinocytes (GSE36287) and skin dermal fibroblasts (GSE34308).

Table S3 Further training samples of unstimulated keratinocytes, skin dermal fibroblasts and others.



THIS ADVERT CONTAINS PROMOTIONAL CONTENT FROM UCB AND IS INTENDED FOR HCPs IN GREAT BRITAIN ONLY

THE OPPORTUNITY FOR COMPLETE, FAST AND LASTING SKIN CLEARANCE^{1,2}

68.2% achieved PASI 100 at Week 16^{†1}

75.9% of patients achieved PASI 75 at Week 4^{†1}

82% of week 16 PASI 100 responders maintained this response up to 3 years²

BIMZELX was well tolerated, the most frequently reported adverse reactions were: upper respiratory tract infections (14.5%, 14.6%, in plaque psoriasis (Pso), and psoriatic arthritis (PsA) respectively) and oral candidiasis (7.3%, 2.3% in Pso, and PsA respectively). Other common reported adverse reactions include Tinea infections, Ear infections, Herpes simplex infections, Oropharyngeal candidiasis, Gastroenteritis, Folliculitis, Headache, Rash, Dermatitis, Eczema, Acne, Injection site reactions, and Fatigue.

Please refer to the SmPC for further information.¹

Challenge expectations in plaque psoriasis^{1,2}

Visit [Bimzelx.co.uk](https://www.bimzelx.co.uk) to discover more.

This site contains promotional information on UCB products.



Stay connected with UCB by scanning the QR code and set your digital preferences.



Use this QR code to access [Bimzelx.co.uk](https://www.bimzelx.co.uk)

This is a promotional UCB website

Footnotes: [†]co-primary endpoints PASI 90 and IGA 0/1 at Week 16

Pso - Plaque Psoriasis; PsA - Psoriatic Arthritis

BIMZELX® (Bimekizumab) is indicated for the treatment of moderate to severe plaque psoriasis in adults who are candidates for systemic therapy. Bimzelx, alone or in combination with methotrexate, is indicated for the treatment of active psoriatic arthritis in adults who have had an inadequate response or who have been intolerant to one or more disease-modifying antirheumatic drugs (DMARDs). Please refer to the SmPC for further information.¹

PRESCRIBING INFORMATION FOR HCP'S IN GREAT BRITAIN

BIMZELX® ▼ (Bimekizumab) is indicated for the treatment of moderate to severe plaque psoriasis in adults who are candidates for systemic therapy, and for active psoriatic arthritis in adults who have had an inadequate response or who have been intolerant to one or more disease-modifying antirheumatic drugs (DMARDs), alone or in combination with methotrexate.¹ (Please consult the Summary of Product Characteristics (SmPC) before prescribing).

Active Ingredient: Bimekizumab – solution for injection in pre-filled syringe or pre-filled pen: 160 mg of bimekizumab in 1 mL of solution (160mg/mL). **Indications:** Moderate to severe plaque psoriasis in adults who are candidates for systemic therapy. Alone or in combination with methotrexate, for active psoriatic arthritis in adults who have had an inadequate response or intolerant to one or more disease-modifying antirheumatic drugs (DMARDs). Adults with active non-radiographic axial spondyloarthritis with objective signs of inflammation as indicated by elevated C-reactive protein (CRP) and/or magnetic resonance imaging (MRI) who have responded inadequately or are intolerant to non-steroidal anti-inflammatory drugs (NSAIDs). Adults with active ankylosing spondylitis who have responded inadequately or are intolerant to conventional therapy.

Dosage and Administration: Should be initiated and supervised by a physician experienced in the diagnosis and treatment of conditions for which Bimzelx is indicated. **Recommended dose:** Plaque Psoriasis: 320 mg (given as two subcutaneous injections of 160 mg each) at week 0, 4, 8, 12, 16 and every 8 weeks thereafter. Psoriatic arthritis: 160 mg (given as 1 subcutaneous injection of 160 mg) every 4 weeks. For psoriatic arthritis patients with coexistent moderate to severe plaque psoriasis, the recommended dose is the same as for plaque psoriasis. After 16 weeks, regular assessment of efficacy is recommended and if a sufficient clinical response in joints cannot be maintained, a switch to 160 mg every 4 weeks can be considered. Axial spondyloarthritis (nr-axSpA and AS): 160 mg (given as 1 subcutaneous injection) every 4 weeks. For patients with plaque psoriasis (including psoriatic arthritis with coexistent moderate to severe psoriasis) and a body weight ≥ 120 kg who did not achieve complete skin clearance at week 16, 320 mg every 4 weeks after week 16 may further improve treatment response. Consider discontinuing if no improvement by 16 weeks of treatment. Renal or hepatic impairment: No dose adjustment needed. Elderly:

No dose adjustment needed. Administer by subcutaneous injection to thigh, abdomen or upper arm. Rotate injection sites and do not inject into psoriatic plaques or skin that is tender, bruised, erythematous or indurated. Do not shake pre-filled syringe or pre-filled pen. Patients may be trained to self-inject. **Contraindications:** Hypersensitivity to bimekizumab or any excipient; Clinically important active infections (e.g. active tuberculosis). **Warnings and Precautions:** Record name and batch number of administered product. **Infection:** Bimekizumab may increase the risk of infections e.g. upper respiratory tract infections, oral candidiasis. Caution when considering use in patients with a chronic infection or a history of recurrent infection. Must not be initiated if any clinically important active infection until infection resolves or is adequately treated. Advise patients to seek medical advice if signs or symptoms suggestive of an infection occur. If a patient develops an infection, the patient should be carefully monitored. If the infection becomes serious or is not responding to standard therapy do not administer bimekizumab until infection resolves. **TB:** Evaluate for TB infection prior to initiating bimekizumab – do not give if active TB. While on bimekizumab, monitor for signs and symptoms of active TB. Consider anti-TB therapy prior to bimekizumab initiation if past history of latent or active TB in whom adequate treatment course cannot be confirmed. **Inflammatory bowel disease:** Bimekizumab is not recommended in patients with inflammatory bowel disease. Cases of new or exacerbations of inflammatory bowel disease have been reported. If inflammatory bowel disease signs/symptoms develop or patient experiences exacerbation of pre-existing inflammatory bowel disease, discontinue bimekizumab and initiate medical management. **Hypersensitivity:** Serious hypersensitivity reactions including anaphylactic reactions have been observed with IL-17 inhibitors. If a serious hypersensitivity reaction occurs, discontinue immediately and treat. **Vaccinations:** Complete all age appropriate immunisations prior to bimekizumab initiation. Do not give live vaccines to bimekizumab patients. Patients may receive inactivated or non-live vaccinations. **Interactions:** A clinically relevant effect on CYP450 substrates with a narrow therapeutic index in which the dose is individually adjusted e.g. warfarin, cannot be excluded. Therapeutic monitoring should be considered. **Fertility, pregnancy and lactation:** Women of child-bearing potential should use an effective method of contraception during treatment and for at

least 17 weeks after treatment. Avoid use of bimekizumab during pregnancy. It is unknown whether bimekizumab is excreted in human milk, hence a risk to the newborn/infant cannot be excluded. A decision must be made whether to discontinue breast-feeding or to discontinue/abstain from Bimzelx therapy. No data available on human fertility. **Driving and use of machines:** No or negligible influence on ability to drive and use machines. **Adverse Effects:** Refer to SmPC for full information. Very Common ($\geq 1/10$): upper respiratory tract infection; Common ($\geq 1/100$ to $< 1/10$): oral candidiasis, tinea infections, ear infections, herpes simplex infections, oropharyngeal candidiasis, gastroenteritis, folliculitis; headache, rash, dermatitis and eczema, acne, injection site reactions, fatigue; Uncommon ($\geq 1/1,000$ to $< 1/100$): mucosal and cutaneous candidiasis (including oesophageal candidiasis), conjunctivitis, neutropenia, inflammatory bowel disease. Storage precautions: Store in a refrigerator (2°C – 8°C), do not freeze. Keep in outer carton to protect from light. Bimzelx can be kept at up to 25°C for a single period of maximum 25 days with protection from light. Product should be discarded after this period or by the expiry date, whichever occurs first.

Legal Category: POM

Marketing Authorisation Numbers: PLGB 00039/0802 (Pre-filled Syringe), PLGB 00039/0803 (Pre-filled Pen).

UK NHS Costs: £2,443 per pack of 2 pre-filled syringes or pens of 160 mg each.

Marketing Authorisation Holder: UCB Pharma Ltd, 208 Bath Road, Slough, Berkshire, SL1 3WE, United Kingdom.

Further information is available from: UCB Pharma Ltd, 208 Bath Road, Slough, Berkshire, SL1 3WE. Tel: 0800 2793177 Email: ucbcares.uk@ucb.com

Date of Revision: August 2023 (GB-P-BK-AS-2300047)

Bimzelx is a registered trademark.

Adverse events should be reported. Reporting forms and information can be found at <http://www.mhra.gov.uk/yellowcard>. Adverse events should also be reported to UCB Pharma Ltd at ucbcares.uk@ucb.com or 0800 2793177.

References: 1. BIMZELX (bimekizumab) SmPC. Available at: <https://www.medicines.org.uk/emc/product/12834/smcp>.

Accessed September 2023 2. Strober et al. [BE BRIGHT open label extension] Br J Dermatol. 2023. 188(6): 749-759.

GB-BK-2300081 Date of preparation: September 2023.

© UCB Biopharma SRL, 2023. All rights reserved.

BIMZELX® is a registered trademark of the UCB Group of Companies.



Inspired by patients.
Driven by science.

Design code 0001